

NJC

Accepted Manuscript



This is an *Accepted Manuscript*, which has been through the Royal Society of Chemistry peer review process and has been accepted for publication.

Accepted Manuscripts are published online shortly after acceptance, before technical editing, formatting and proof reading. Using this free service, authors can make their results available to the community, in citable form, before we publish the edited article. We will replace this *Accepted Manuscript* with the edited and formatted *Advance Article* as soon as it is available.

You can find more information about *Accepted Manuscripts* in the [Information for Authors](#).

Please note that technical editing may introduce minor changes to the text and/or graphics, which may alter content. The journal's standard [Terms & Conditions](#) and the [Ethical guidelines](#) still apply. In no event shall the Royal Society of Chemistry be held responsible for any errors or omissions in this *Accepted Manuscript* or any consequences arising from the use of any information it contains.

Three N-stabilization rhodamine-based fluorescent probes for Al³⁺ via Al³⁺-promoted hydrolysis of Schiff base

Peigang Ding^a, Jinhui Wang^a, Junye Cheng^a,
Yufen Zhao^{a,c} and Yong Ye^{a,c,*}

Received (in XXX, XXX) Xth XXXXXXXXX 20XX, Accepted
Xth XXXXXXXXX 20XX

DOI: 10.1039/b000000x

New fluorescent probes L1-L3 displayed high sensitivity toward Al³⁺

Introduction

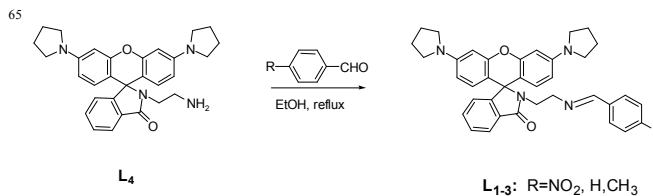
As is known to all, aluminum is the third most abundant element in the earth's crust. It widely exists in the environment due to acidic rain and is considered to be toxic in biological activities.¹⁻³ Regarding toxicological effects of aluminum, its primary targets are different from those of heavy metals.⁴ The widespread use of aluminum in water treatment, as a food additive, and in many industrial activities including the manufacturing of cars and computers often exposes people to this metal.^{5,6} Excessive exposure of the human body to Al³⁺ leads to the malfunction of central nervous system such as Alzheimer's disease and Parkinson's disease.^{7,8} The WHO recommended the average daily human intake of Al³⁺ of around 3–10 mg and weekly tolerable dietary intake as 7 mg kg⁻¹ body weight. Therefore, trace level determination of Al³⁺ is highly important.

In the last decade, many methods such as graphite furnace atomic absorption spectrometry, atomic emission spectrometry, inductively coupled plasma atomic emission spectrometry and electrochemical methods have been used for aluminum detection. All of these techniques are generally time-consuming and expensive as well. In contrast, optical detection via fluorescence is an operationally easy technique besides being highly sensitivity. Due to great changes in the absorption and/or fluorescent spectra of many organic molecules after coordinating with ions, colorimetric and fluorescence analytical methods are very good and effective ways to detect metal ions.⁹⁻¹⁵

The rhodamine moiety has been used widely in the field of chemosensors, especially as a chemodosimeter, given its fluorescence off-on behavior that results from its particular structural properties. Upon metal binding, its structure can undergo a change from the spirolactam to an open ring amide, resulting in a magenta-colored, highly fluorescent compound¹⁶.

While some rhodamine-based chemosensors for Al³⁺ ions have been reported to date¹⁷⁻²⁶, dual colorimetric and fluorescent chemosensors for Al³⁺ were still rare and some of them were not efficient enough to be selective toward Al³⁺ or sensed it in organic solvents. Therefore, developing sensors which are able to detect Al³⁺ by both fluorescence and naked eye in aqueous solution are very valuable. In this paper, we report three new N-stabilization rhodamine-based fluorescent probes which exhibited sensitive detection toward Al³⁺ via significant fluorescence enhancement in solution, and, at the same time, showed a significant color change from colorless to red. Similar structures had been designed to compounds L₁, L₂ and L₃. By comparing with each other, we could know that the different electronic distribution among the chemodosimeters' structures had great

influence in their recognition toward Al³⁺. Own to more stable structure, L₁ shown the best sensing property, so we selected L₁ as a representation example to expatiate in the following discussion. To the best of our knowledge, none of rhodamine-based probes which fluorescent mechanism is based on the Al³⁺-promoted hydrolysis of the Schiff base has been reported for detection of Al³⁺ up to now.



Scheme 1. Synthetic route of target compounds.

Experimental

Apparatus

Fluorescence spectra measurements were performed on a HITACHI F-4500 fluorescence spectrophotometer, and the excitation and emission wavelength band passes were both set at 5.0 nm. Absorption spectra were measured on a UV-2102 double-beam UV/VIS spectrometer, Perkin Elmer precisely. NMR spectra were recorded on a Bruker DTX-400 spectrometer in CDCl₃, using TMS as internal standard. Mass spectral determination was carried on a HPLC Q-T of HR-MS.

Materials

All the materials for synthesis were purchased from commercial suppliers and used without further purification. The solutions of metal ions were prepared from their nitrate salts, except for FeCl₃, FeCl₂, CrCl₃ and MnCl₂. The metal ions were prepared as 10.00 mM in water solution.

Syntheses

As shown in Scheme 1, the compounds L₁₋₃ were prepared by reacting L₄ with aromatic aldehyde. L₄ was synthesized according to literature.²⁷

L₁

L₄ (0.5 mmol, 0.24 g) was dissolved in 25 mL ethanol, and then p-nitrobenzaldehyde (1 mmol, 0.15 g) was slowly added. The mixture was stirred and refluxed for 12 h at 80 °C. After distillation in vacuum, the residue was recrystallized with methanol and water to give the final product L₁ in yield of 78.4%. ¹H NMR (400 MHz, CDCl₃, δ ppm): 8.17 (d, *J* = 8.0 Hz, 2H), 8.06 (s, 1H), 7.91-7.90 (m, 1H), 7.72 (d, *J* = 8.4 Hz, 2H), 7.43 (s, 1H), 7.03 (d, *J* = 4.0 Hz, 1H), 6.44 (d, *J* = 8.4 Hz, 1H), 6.28 (s, 2H), 6.14-6.12 (m, 1H), 3.52-3.49 (m, 1H), 3.25 (s, 8H), 1.99 (s, 8H); ¹³C NMR (100 MHz, CDCl₃, δ ppm): 168.5, 159.8, 153.9, 153.1, 148.8, 148.7, 141.7, 132.6, 130.9, 128.9, 128.8, 128.1, 123.7, 123.6, 122.8, 108.4, 105.7, 98.0, 65.2, 59.3, 47.6, 41.1, 25.5. HR-MS: C₃₇H₃₅N₅O₄ [M+H]⁺, calcd for 614.2762. Found: 614.2767. (Supporting Information, Figs. S1–S3);

L₂

Compound L₂ was prepared using a general procedure which is essentially similar to that used for L₁. Yield of L₂: 69.3%. ¹H NMR (400 MHz, CDCl₃, δ ppm): 8.01 (s, 1H), 7.92-7.90 (m, 1H), 7.58-7.56 (m, 2H), 7.44-7.39 (m, 2H), 7.36-7.31 (m, 3H), 7.05-7.03 (m, 1H), 6.46 (d, *J* = 8.8 Hz, 2H), 6.29 (s, 2H), 6.16-6.14 (m, 2H), 3.44 (s, 4H), 3.25 (t, *J* = 3.2 Hz, 8H), 2.01-1.98 (m, 8H); ¹³C NMR (100 MHz, CDCl₃, δ ppm): 168.4, 162.4, 154.0, 153.1, 148.7, 132.4, 130.4, 128.9, 128.4, 128.1, 128.0, 123.7, 122.8, 108.4, 105.8, 98.0, 65.1, 59.0, 47.6, 41.3, 25.5. HR-MS: C₃₇H₃₆N₄O₂ [M+H]⁺, calcd for 569.2911. Found: 569.2910. (Supporting Information, Figs. S4–S6).

L_3

The following compound was prepared using a general procedure which is essentially similar to that used for L_1 . Yield of L_3 : 62.7%. ^1H NMR (400 MHz, CDCl_3 , δ ppm): 8.03 (s, 1H), 7.94-7.93 (m, 1H), 7.49 (d, $J = 7.6$ Hz, 2H), 7.45-7.43 (m, 2H), 7.15 (d, $J = 7.6$ Hz, 2H), 7.07-7.05 (m, 1H), 6.49 (d, $J = 8.8$ Hz, 2H), 6.32 (s, 2H), 6.17 (d, $J = 8.4$ Hz, 2H), 3.77-3.71 (m, 4H), 3.46-3.29 (m, 8H), 2.36 (s, 3H), 2.02 (s, 8H); ^{13}C NMR (100 MHz, CDCl_3 , δ ppm): 168.3, 162.3, 154.1, 153.1, 148.7, 140.6, 133.7, 132.4, 131.1, 129.1, 128.9, 128.1, 127.9, 123.7, 122.8, 108.4, 105.8, 98.0, 65.1, 59.0, 47.6, 41.3, 25.5, 21.5. HR-MS: $\text{C}_{38}\text{H}_{38}\text{N}_4\text{O}_2$ $[\text{M}+\text{H}]^+$, calcd for 583.3068. Found: 583.3074. (Supporting Information, Figs. S7–S9).

Results and discussion

The structure of title compounds L_1 , L_2 and L_3 were characterized by ^1H NMR, ^{13}C NMR and HR-MS. The results were in good agreement with the structure showed in Scheme 1. Fluorescence and UV–vis studies were performed using a 10 μM solution of L_1 , L_2 and L_3 in a $\text{CH}_3\text{CN}/\text{H}_2\text{O}$ (95:5, v/v) solution with appropriate amounts of metal ions. Solutions were shaken for 120 min before measuring the absorption and fluorescence in order to make the metal ions chelate with the sensors sufficiently.

Steady-state optical properties

Compared with $L_2+\text{Al}^{3+}$ and $L_3+\text{Al}^{3+}$, $L_1+\text{Al}^{3+}$ had higher fluorescence quantum yield (Fig. S10). This means that the strong electron withdrawing group on benzene benefiting to the chelate of Al^{3+} with sensors. The effect of the reaction media for the binding of L_1 with Al^{3+} was studied, and the results were shown in Fig S11. It was found that solvent have great effect on the coordination reaction. When the coordination reaction was performed in acetonitrile–water solution, high F/F_0 and ΔA values were obtained, indicating that acetonitrile–water media is favorable for fluorescent measurement. Therefore, acetonitrile–water solution was selected for fluorescent assay and the colorimetric assay, respectively. As shown in Fig. 1, L_1 exhibited a 190-fold enhancement of fluorescence intensity at peak wavelength $\lambda_{\text{max}}=582$ nm in the presence of 10 equiv. Al^{3+} , so we selected L_1 as the representation when expatiating the characters of the three compounds in the following discussion.

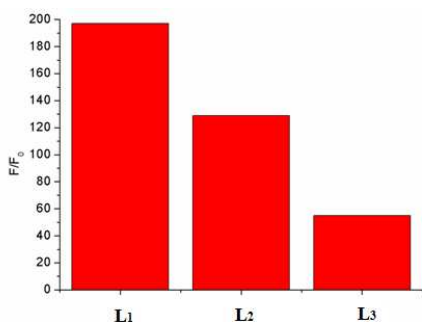


Fig. 1. F/F_0 : Fluorescence intensity (at 582 nm) of L_1 , L_2 and L_3 (10 μM) in $\text{CH}_3\text{CN}/\text{H}_2\text{O}$ (95/5, v/v) with the presence of Al^{3+} (100 μM) ($\lambda_{\text{ex}} = 520$ nm); F_0 : Fluorescence intensity (at 582 nm) of L_1 , L_2 and L_3 (10 μM) only in $\text{CH}_3\text{CN}/\text{H}_2\text{O}$ (95/5, v/v) ($\lambda_{\text{ex}} = 520$ nm).

UV–vis spectral responses of L_1

As shown in Fig. 2, UV–vis spectrum of compound L_1 (10 μM) exhibited only very weak bands over 400 nm. Addition of 10 equiv. Al^{3+} into solution immediately resulted in a significant

enhancement of absorbance at about 562 nm simultaneously the color changed into red. Under the identical condition, no obvious response could be observed upon the addition of other ions including Zn^{2+} , Mg^{2+} , Ca^{2+} , Cd^{2+} , Cu^{2+} , Pb^{2+} , Hg^{2+} , Ba^{2+} , Ni^{2+} , Fe^{2+} , Mn^{2+} , K^+ , Li^+ , Ag^+ , Co^{2+} and Na^+ except for Fe^{3+} and Cr^{3+} , which caused a mild effect compared to Al^{3+} . This interesting feature demonstrated that compound L_1 can serve as a selective “naked-eye” chemosensor for Al^{3+} .

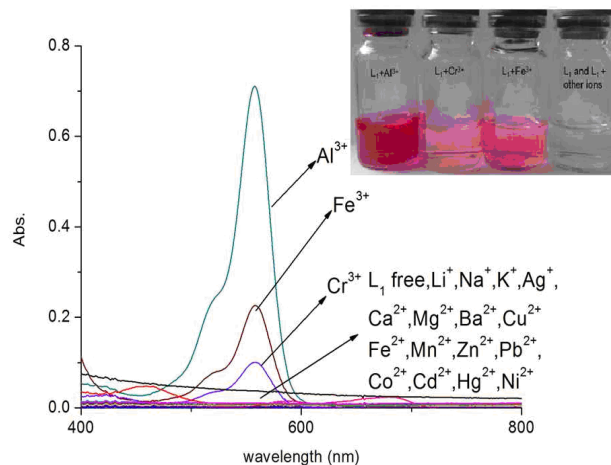


Fig. 2. Absorbance spectra of L_1 (10 μM) in $\text{CH}_3\text{CN}/\text{H}_2\text{O}$ (95:5, v/v) solution with the presence of 10 equiv. of various species. Inset: the photos of L_1 with different metal ions in $\text{CH}_3\text{CN}/\text{H}_2\text{O}$ (95:5, v/v) solution.

To further investigate the interaction of Al^{3+} and L_1 , an ultraviolet titration experiment was carried out (Fig. 3). The Al^{3+} binding stoichiometry of L_1 can be determined from titration and the Job plot²⁸. A plot of $[\text{Al}^{3+}]/\{[\text{Al}^{3+}] + [\text{L}_1]\}$ versus the molar fraction of Al^{3+} was provided in Fig. 4. The absorbance reached a maximum when the ratio was 0.5, indicating a 1:1 stoichiometry of the Al^{3+} to L_1 in the complex.

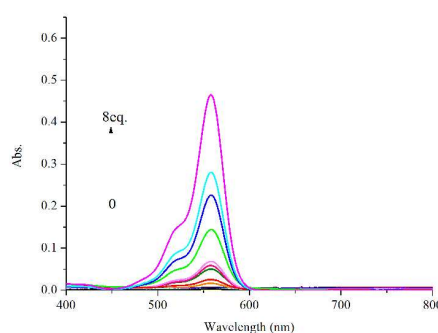


Fig. 3. Absorbance spectra of L_1 (10 μM) in $\text{CH}_3\text{CN}/\text{H}_2\text{O}$ (95:5, v/v) upon addition of different amounts of Al^{3+} ions.

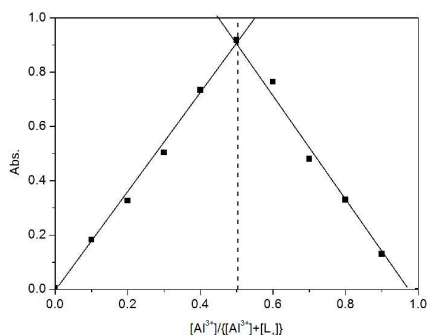


Fig. 4. Job's plots of the complexation between L_1 and Al^{3+} . Total concentration of L_1+Al^{3+} was kept constant at 100 μM .

Fluorescence spectral responses of L_1

As shown in **Fig. 5**, L_1 exhibited a very weak fluorescence in the absence of metal ions. When 10 equiv. Al^{3+} was introduced to a 10 μM solution of L_1 in CH_3CN/H_2O (95:5, v/v), a remarkably enhancement of fluorescence spectra was observed. The fluorescence enhancement of Al^{3+} to compound L_1 was as high as 190-fold. Under the same condition, a mild fluorescence enhancement factors was also detected for Fe^{3+} and Cr^{3+} , but Zn^{2+} , Mg^{2+} , Ca^{2+} , Cd^{2+} , Cu^{2+} , Pb^{2+} , Hg^{2+} , Ba^{2+} , Ni^{2+} , Fe^{2+} , Mn^{2+} , K^+ , Li^+ , Ag^+ , Co^{2+} and Na^+ showed no obvious changes on fluorescence intensity and color. From fluorescence spectra of L_2 and L_3 , we could know Fe^{3+} and Cr^{3+} had more interference (**Fig. 6-7**). Probe L_1 had better fluorescence property. It may benefit from the strong electron withdrawing group. Moreover, we also confirmed the competitive experiments that the background metal ions showed very low interference with the detection of in Al^{3+} water solution (**Fig. 8**). Generally, the detection limit of metal ions is needed for fluorescence sensor. Under optical conditions, the linear response for the fluorescence intensity response of compound L_1 was between 8 and 18 μM (**Fig. 9**), and the detection limit of Al^{3+} was measured to be 3.98 μM .

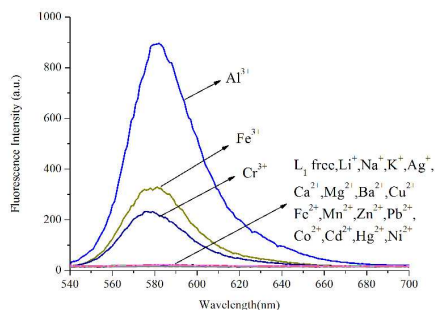


Fig. 5. Fluorescence spectra of L_1 (10 μM) in CH_3CN/H_2O (95:5, v/v) with the presence of 10 equiv. of various metal ions ($\lambda_{exc} = 520$ nm, slit = 5 nm).

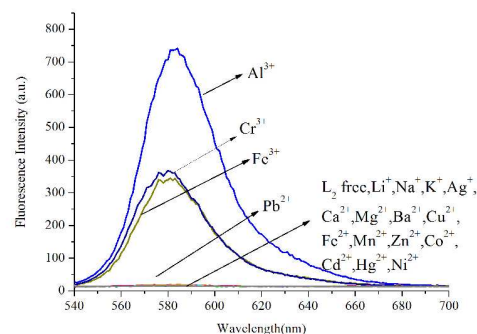


Fig. 6. Fluorescence spectra of L_2 (10 μM) in CH_3CN/H_2O (95:5, v/v) with the presence of 10 equiv. of various metal ions ($\lambda_{exc} = 520$ nm, slit = 5 nm).

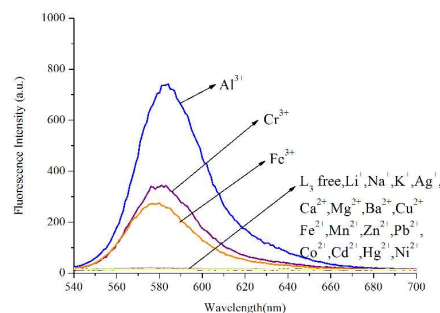


Fig. 7. Fluorescence spectra of L_3 (10 μM) in CH_3CN/H_2O (95:5, v/v) with the presence of 10 equiv. of various metal ions ($\lambda_{exc} = 520$ nm, slit = 5 nm).

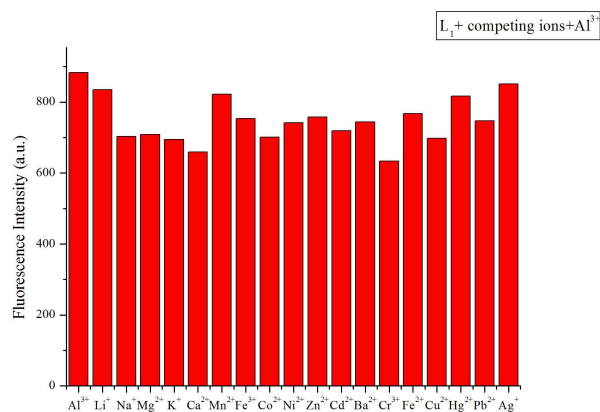


Fig. 8. Fluorescence intensity (at 582 nm) of L_1 upon the addition of 100 μM Al^{3+} in the presence of 100 μM background metal ions in CH_3CN/H_2O (95/5, v/v) ($\lambda_{exc} = 520$ nm, slit = 5 nm).

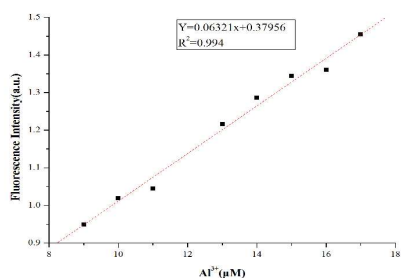


Fig. 9. The fluorescence intensity (at 582 nm) of compound **L**₁ (10 μM) as a function of the Al³⁺ concentration in CH₃CN/H₂O (95/5, v/v) solution (λ_{ex} = 520 nm, slit = 5 nm).

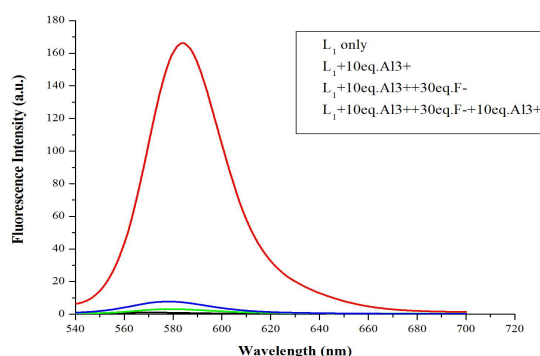


Fig. 10. Fluorescence intensity (at 582 nm) of **L**₁ (10 μM) to Al³⁺ in CH₃CN/H₂O (95:5, v/v) solutions (1) Baseline: 10 μM **L**₁ only; (2) red line: 10 μM **L**₁ with 10 equiv. Al³⁺; (3) green line: 10 μM **L**₁ with 10 equiv. Al³⁺ and then addition of 30 equiv. F⁻; (4) blue line: 10 μM **L**₁ with 10 equiv. Al³⁺ and 30 equiv. F⁻ then addition of 10 equiv. Al³⁺ (λ_{ex} = 520 nm, slit = 5 nm).

Mechanism

To investigate the Al³⁺ enhancement mechanism, IR spectra of **L**₁ and **L**₁ + Al³⁺ were taken in KBr disks (Fig.S15.). The peak at 1694 cm⁻¹, which corresponds to the amide carbonyl absorption disappeared upon with the addition of Al³⁺. This supported the notion that the carbonyl group of **L**₁ is involved in the coordination of metal ions.

In addition, the F⁻-adding experiments were conducted to examine the reversibility of this reaction and the result was shown in Fig. 10. When F⁻ (3 equiv. of Al³⁺) was added to the **L**₁ + Al³⁺ CH₃CN/H₂O solution, the fluorescence intensity at 582 nm was decreased (green line) and further addition of 10 equiv. Al³⁺ could not recover the fluorescence (blue line). To investigate the fluorescence quenching mechanism, the ¹H NMR spectra of the complex of **L**₁ + Al³⁺ was operated. As it was seen from Fig. 11, a new single peak was observed at 10.2 ppm when Al³⁺ was added to **L**₁. Comparing the ¹H NMR spectra of p-nitrobenzaldehyde with ¹H NMR spectra of the complex of **L**₁ + Al³⁺, it can be confirmed that the new single peak is belong to the aldehyde proton (H_a) of p-nitrobenzaldehyde (Fig. S12). The HR-MS of **L**₁ + Al³⁺ in CH₃CN/H₂O (95/5, v/v) was also conducted (Fig. S13). An unique peak at m/z 481.2602 corresponding to [**L**₆ + H]⁺ was clearly observed when 1 equiv. of Al³⁺ was added to **L**₁, whereas **L**₁ without Al³⁺ exhibited peaks only at m/z 614.2

which corresponded to [**L**₁ + H]⁺ (Fig.S3). The form of **L**₆-Al³⁺ complex was also confirmed by ESI-MS analysis. As shown in Fig.S14, the [M+H]⁺ of **L**₆ appeared at m/z 481.4. When 1 equiv. of Al³⁺ was added to **L**₁ in H₂O/CH₃CN, the ESI-MS spectra showed the peak of **L**₆-Al³⁺ complex. The signal at m/z 629.4 (calculated value, 629.4) correspond to [**L**₆+Al³⁺+2HCOO⁻+CH₃OH]⁺. Both UV-vis and fluorescence data lead to a significant OFF-ON signal. From the molecular structure and spectral results of **L**₁, an irreversible fluorescent chemodosimeters for Al³⁺ was constructed as shown in Scheme 2. Firstly, the addition of the Al³⁺ ion induced a ring opening of the spirolactam of rhodamine took place. Then, **L**₁-Al was hydrolyzed into p-nitrobenzaldehyde. And it was certified by theoretical calculation (the data was supplied in Supporting Information). The DFT calculations were performed using the Gaussian 09 program^[29]. The structures of **L**₅, **H**₂O, **L**₆ and p-nitrobenzaldehyde were optimized at the B3LYP^[30-32]/6-31G(d) level in acetonitrile solvent, using the integral equation formalism polarizable continuum model (IEF-PCM)^[33-34]. The calculated results demonstrate that the free energies of **L**₆ and p-nitrobenzaldehyde is 14.7 kcal/mol lower than those of **L**₅ and **H**₂O, indicating that this hydrolysis step is an exothermic process. So in the reaction, **L**₅ tends to hydrolyze to **L**₆ (Fig.12.). From Fig.5, we know that both Cr³⁺ and Fe³⁺ can induce the moderate fluorescence enhancements to **L**₁. The mechanism of **L**₁ with Fe³⁺ and Cr³⁺ were thought to be similar to that of **L**₁ with Al³⁺. ¹H NMR spectra of the complex of **L**₁ + Fe³⁺ and **L**₁ + Cr³⁺ was operated (Fig. S16 and Fig. S18). The same new single peak was observed at 10.179ppm and 10.138ppm, respectively. The ESI mass spectra of **L**₁+Fe³⁺ and **L**₁+Cr³⁺ in CH₃CN/H₂O (95/5, v/v) was conducted (Fig. S17 and Fig. S19) and similar hydrolysis product was found. A kind of Fe³⁺-induced Schiff base hydrolysis mechanism has been reported by Kim and coworkers³⁵.

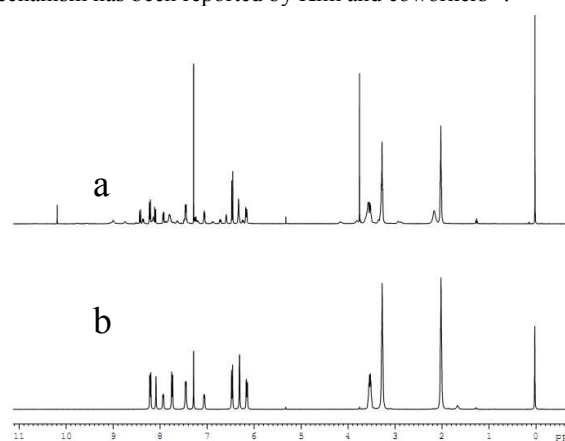
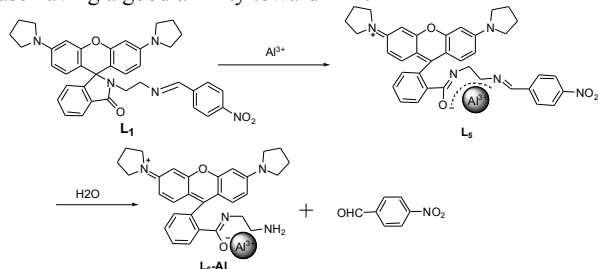


Fig. 11. ¹H NMR spectra of **L**₁ + Al³⁺ (a) and **L**₁ (b) in CDCl₃.

In order to investigate the influence of the different acid concentration on the spectra of **L**₁ and find a suitable pH span in which **L**₁ can selectively detect Al³⁺ efficiently, the acid titration experiments were performed. The addition of Al³⁺ led to the fluorescence enhancement over a wide pH range (1.0–8.0), which is attributed to opening of the rhodamine spirolactam structure (Fig.S20). Moreover, a time course of the fluorescence response of **L**₁ upon addition of Al³⁺ was shown in Fig.S21. The kinetics of fluorescence enhancement at 593 nm by the newly developed fluorescent probe was recorded. It indicated that this reaction between **L**₁ and Al³⁺ was slow. And, the recognizing event of **L**₁ with Fe³⁺ could complete in 80 minutes (Fig.S22). The chemodosimeters **L**₂ and **L**₃ show similar properties as **L**₁ (see supporting information Figs. S23–S34). The detection

limits of L2 and L3 were measured to be 32 μM (Fig. S27) and 49 μM (Fig. S34). The three chemodosimeters exhibit irreversible, selective and sensitive recognition toward Al^{3+} over other metal ions. The colorimetric and fluorometric responses between the sensors L1-L3 and Al^{3+} can also be conveniently detected by the naked eye. The fluorescence enhancement of Al^{3+} to L1, L2 and L3 is as high as 190, 120 and 60-fold, respectively. These indicate the differences among the three chemodosimeters' structures have great influence in their recognition toward Al^{3+} . Due to the strong electron withdrawing group on benzene ring that result in Schiff base having a good affinity toward Al^{3+} .



Scheme 2. Possible sensing mechanism of L1 with Al^{3+} .

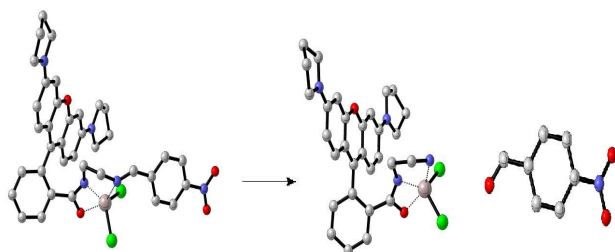


Fig. 12. Calculated energy-minimized structure of L5, L6 and p-nitrobenzaldehyde (gray: C atoms; blue: N atoms; red: O atoms; green: Cl; brown: Al^{3+}).

Many fluorescent sensors for Al^{3+} detection could only be performed in solution, which would limit their applications under special circumstances such as on-site detection *in situ*. To demonstrate the practical application of our sensor, we prepared the test papers of sensor L1. It was easily prepared by immersing a filter paper into the solution of L1 in CH_2Cl_2 (1 mM) and then drying in air. Next, to different Al^{3+} concentration solutions (0, 1.0×10^{-4} M, 1.0×10^{-3} M, 1.0×10^{-2} M), these strips were immersed for 5 s and taken out of the solution. As depicted in Fig. 13, the color of the test paper changed from colorless to purple and deepened gradually with the increasing of Al^{3+} concentration. These paper-made test kits may be used as a simple tool for detecting Al^{3+} in environmental samples. To validate its practicality in real environmental samples, we employed probe L1 in a standard addition method³⁶⁻³⁸ to determine Al^{3+} concentrations in water samples from Jinshui River (in Zhengzhou, Henan province, China), no fluorescence enhancement was observed. When the water samples were spiked with different Al^{3+} concentrations (25 μM , 50 μM , and 100 μM) and measured with the current methods, Al^{3+} recoveries were about 20% (Table S1).

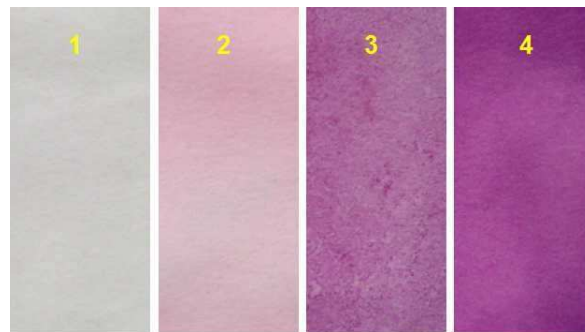


Fig. 13 Photographs of the test kits with L1 for detecting Al^{3+} in ($\text{CH}_3\text{CN}/\text{H}_2\text{O} = 95:5$, v/v) solution with different concentrations: (1) 0; (2) 1.0×10^{-4} M; (3) 1.0×10^{-3} M; (4) 1.0×10^{-2} M.

45 Conclusions

In summary, we synthesized three fluorescent chemodosimeters L1, L2 and L3. The colorimetric and fluorescent response to Al^{3+} can be conveniently detected even by the naked eye, which provides a facile method for visual detection of Al^{3+} . Theoretical calculation indicated that the electronic distribution of the N atom of C=N is -0.436, -0.46 and -0.464, respectively (log file). Own to the strong electron withdrawing group on benzene, the Schiff base L1 changed stable, which was favor for high sensitivity for the detection of Al^{3+} . As we know, higher electronegativity of N atom of C=N of Schiff base is easier to hydrolyze. Furthermore, the mechanism of fluorescence was found to be the aluminum complexation with rhodamine and subsequent Al^{3+} -promoted hydrolysis of the Schiff base. Also, Iron and chromium complexation had the same hydrolysis mechanism. The simple and convenient test paper may provide an easy way to detect Al^{3+} in our daily life.

Acknowledgments

This work was financially supported by the National Science Foundation of China (No. 21375113) and Program for New Century Excellent Talents in University (NCET-11-0950).

Notes and references

- ^a Phosphorus Chemical Engineering Research Center of Henan Province, the College of Chemistry and Molecular Engineering, Zhengzhou University, Zhengzhou 450052, China. Fax: 86 371 67767051; Tel: 86 371 67767050; E-mail: yeyong03@tsinghua.org.cn
 - ^b Department of Chemistry and Key Laboratory for Chemical Biology of Fujian Province, Xiamen University, Xiamen 361005, China
 - ^c Key Laboratory of Bioorganic Phosphorus Chemistry & Chemical Biology (Ministry of Education), Department of Chemistry, Tsinghua University, Beijing 100084, China
- † Electronic Supplementary Information (ESI) available: [details of any supplementary information available should be included here]. See DOI: 10.1039/b000000x/
- ‡ * Corresponding author.
- 1 T. P. Flaten, M. degard, *Food. Chem. Toxicol.*, 1988, **26**, 959.
 - 2 J. Ren, H. Tian, *Sensors*, 2007, **7**, 3166.
 - 3 R. A. Yokel, *Neurotoxicology*, 2000, **21**, 813
 - 4 G. Muller, V. Bernuzzi, D. Desor, M. F. Hutin, D. Burnel, P.R. Lehr, *Teratology*, 1990, **42**, 253.
 - 5 J. Barceló, C. Poschenrieder, *Environ. Exp. Bot.*, 2002, **48**, 75.
 - 6 Z. Krejpcio, R.W. Wojciak, *P. J. Environ. Stud.*, 2002, **11**, 251.
 - 7 D. P. Perl, D. C. Gajdusek, R. M. Garruto, R. T. Yanagihara, C. J. Gibbs, *Science*, 1982, **217**, 1053.

- 8 D. P. Perl, A. R. Brody, *Science*, 1980, **208**, 297.
- 9 Y. Chen, K. Y. Han, Y. Liu, *Bioorg. Med. Chem.*, 2007, **15**, 4537.
- 10 R. Partha, D. Koushik, M. Mario, R. Jagnyeswar, B. Pradyot, *Inorg. Chem.*, 2007, **46**, 6405.
- 5 11 M. Royzen, A. Durandin, V.G. Young, N. E. Geacintov, J. W. Canary, *J. Am. Chem. Soc.*, 2006, **128**, 3854.
- 12 A. Banerjee, A. Sahana, S. Das, S. Lohar, S. Guha, B. Sarkar, S. K. Mukhopadhyay, A. K. Mukherjee and D. Das, *Analyst*, 2012, **137**, 2166.
- 10 13 H. Y. Lee, K. M. K. Swamy, J. Y. Jung, G. Kim, J. Yoon, *Sensor. Actuat. B-chem.*, 2013, **182**, 530.
- 14 S. Sen, T. Mukherjee, B. Chattopadhyay, A. Moirangthem, A. Basu, J. Marekd and P. Chattopadhyay, *Analyst*, 2012, **137**, 3975.
- 15 15 R. Patil, A. Moirangthem, R. Butcher, N. Singh, A. Basu, K. Tayade, U. Fegade, D. Hundiware and A. Kuwar, *Dalton Trans.*, 2014, **43**, 2895.
- 16 M. Beija, C. A. M. Afonso, J. M. G. Martinho, *Chem. Soc. Rev.*, 2009, **38**, 2410.
- 17 S. Das, M. Dutta, D. Das, *Anal. Methods*, 2013, **5**, 6262
- 20 18 C. Y. Li, Y. Zhou, Y. F. Li, C. X. Zou, X. F. Kong, *Sensor. Actuat. B-chem.*, 2013, **186**, 360.
- 19 Y. S. Mi, Z. Cao, Y. T. Chena, S. Long, Q. F. Xie, D. M. Liang, W. P. Zhu, J. N. Xiang, *Sensor. Actuat. B-chem.*, 2014, **192**, 164.
- 20 S. B. Maity, P. K. Bharadwaj, *Inorg. Chem.*, 2013, **52**, 1161.
- 25 21 X. X. Fang, S. F. Zhang, G. Y. Zhao, W. W. Zhang, J. W. Xu, A. M. Ren, C. Q. Wu, W. Yang, *Dyes and Pigments*, 2014, **101**, 58.
- 22 A. Sahana, A. Banerjee, S. Lohar, B. Sarkar, S. K. Mukhopadhyay, D. Das, *Inorg. Chem.*, 2013, **52**, 3627
- 23 C. Lohani, J. Kim, S. Chung, J. Yoon and K. Lee, *Analyst*, 2010, **135**, 2079
- 30 24 Z. Li, Q. Hu, C. Li, J. Dou, J. Cao, W. Chen, Q. Zhu, *Tetrahedron Lett.* 2014, **55**, 1258
- 25 L.Y.Wang, L.L.Yang, D.R. Cao, *Sensors and Actuators B: Chemical*, 2014, **202**, 949
- 35 26 K. Mukhopadhyay, D.A. Safin, M. G. Babashkina, M. Bolte, Y. Garcia, D. Das, *Dalton Trans.*, 2013, **42**, 13311.
- 27 J.H.Wang, D. Zhang, Y.Q. Liu, P.G. Ding, C.C.Wang, Y.Ye, Y.F. Zhao, *Sensors and Actuators B: Chemical*, 2014, **191**, 344.
- 28 C. Y. Huang, *Meth. Enzymol.*, 1982, **87**, 509.
- 40 29 G.W. Trucks, M.J. Frisch, H.B. Schlegel, G.E. Scuseria, M.A. Robb, J.R. Cheeseman, G. Scalmani, V. Barone, B. Mennucci, G.A. Petersson, H. Nakatsuji, M. Caricato, X. Li, H.P. Hratchian, A.F. Izmaylov, J. Bloino, G. Zheng, J.L. Sonnenberg, M. Hada, M. Ehara, K. Toyota, R. Fukuda, J. Hasegawa, M. Ishida, T. Nakajima, Y. Honda, O. Kitao, H. Nakai, T. Vreven, J.A. Montgomery, Jr, J.E. Peralta, F. Ogliaro, M. Bearpark, J.J. Heyd, E. Brothers, K.N. Kudin, V.N. Staroverov, T. Keith, R. Kobayashi, J. Normand, K. Raghavachari, A. Rendell, J.C. Burant, S.S. Iyengar, J. Tomasi, M. Cossi, V. Rega, J.M. Millam, M. Klene, J.E. Knox, J.B. Cross, V. Bakken, C. Adamo, J. Jaramillo, R. Gomperts, R.E. Stratmann, O. Yazyev, A.J. Austin, R. Cammi, C. Pomelli, J.W. Ochterski, R.L. Martin, K. Morokuma, V.G. Zakrzewski, G.A. Voth, P. Salvador, J.J. Dannenberg, S. Dapprich, A.D. Daniels, O. Farkas, J.B. Foresman, J.V. Ortiz, J. Cioslowski, D.J. Fox, Revision C.01; , (2010).
- 55 30 A.D. Becke, *J. Chem. Phys.*, 1993, **98**, 5648.
- 31 C.T. Lee, W.T. Yang, R.G. Parr, *Phys. Rev. B.*, 1988, **37**, 785.
- 32 B. Michlich, A. Savin, H. Stoll, H. Preuss, *Chem. Phys. Lett.*, 1989, **157**, 200.
- 60 33 V. Barone, M. Cossi, *J. Phys. Chem. A*, 1998, **102**, 1995.
- 34 B. Mennucci, J. Tomasi, *J. Chem. Phys.*, 1997, **106**, 5151.
- 35 M. H. Lee, T. V. Giap, S. H. Kim, Y. H. Lee, C.H. Kang, J. S. Kim, *Chem. Commun.*, 2010, **46**, 1407.
- 36 Z. Wang, D.M. Han, W.P. Jia, Q.Z. Zhou, W.P. Deng, *Anal. Chem.* 2012, **84**, 4915–4920.
- 65 37 J. V. Ros-Lis, B. Garcia, D. Jimenez, R. Martinez-Manez, F. Sancenon, J. Soto, F. Gonzalvo, M. C. Valldcabres, *J. Am. Chem. Soc.* 2004, **126**, 4064–4065.
- 38 J. Li, C. F. Zhang, S. H. Yang, W. C. Yang, G. F. Yang, *Anal. Chem.* 2014, **86**, 3037–3042.
- 70